Macromolecules
ARTICLE

Macromolecules **2010**, *43*, 6731–6738 **6731**
DOI: 10.1021/ma1011792

Preparation, Characterization, and Properties of Novel Polyhedral Oligomeric Silsesquioxane−Polybenzimidazole Nanocomposites by Friedel−Crafts Reaction

Yang Liu, Zixing Shi,* Hongjie Xu, Jianhua Fang, Xiaodong Ma, and Jie Yin

School of Chemistry and Chemical Engineering, State Key Laboratory for Metal Matrix Composite Materials Shanghai Jiao Tong University, 800 Dongchuan Road, 200240, Shanghai, People's Republic of China

Received May 28, 2010; Revised Manuscript Received July 8, 2010

ABSTRACT: The organic−inorganic nanocomposites involving OPBI (poly[2,2′-(*p*-oxidiphenylene)-5,5′-bibenzimidazole]) and polyhedral oligomeric silsesquioxane (POSS) were prepared via in situ polymerization of 4,4′-dicarboxydiphenyl ether (DCDPE) and 3,3′-diaminobenzidine (DABz) in the presence of the POSS where the organic group on silsesquioxane cage is phenyl. NMR, XPS, and XRD characterization of POSS-*g*-OPBI, purified from the POSS-*g*-OPBI/OPBI hybrid, revealed that the OPBI chains were successfully attached to the phenyl group of the POSS through Friedel−Crafts (F−C) reaction. The homogeneous dispersion of POSS cages in the polymer matrix was evidenced by SEM. The DMA results showed that the moduli of the POSS-*g*-OPBI/OPBI nanocomposites were significantly higher than OPBI matrix, indicating the nano-reinforcement effect of POSS cages. Thermogravimetric analysis indicated that the thermal stability of the polymer matrix was not sacrificed but improved by introducing a small amount of POSS since POSS showed lower thermal stability than OPBI. More importantly, the mechanical properties, including tensile and yield strength, Young's modulus, and toughness, were obviously simultaneously increased by introducing POSS into the nanocomposite, which is quite differently from the traditional nanocomposites, where the ductility and toughness of polymer were usually reduced substantially upon the incorporation of inorganic reinforced agent.

1. Introduction

Organic−inorganic nanocomposite materials have attracted a great deal of attention recently due to their potential as candidate materials for bridging the gap between organic polymers and inorganic ceramics.[1−4] The nanoscaled distribution of reinforcing agents can optimize the intercomponent interactions and affords the materials with improved properties. Recently, organic/inorganic additives such as polyhedral oligomeric silsesquioxane (POSS) modifiers in polymeric systems have been used to create nanocomposites due to excellent comprehensive properties of POSS-containing hybrid nanocomposites and the simplicity in processing of materials.[5−19]

The POSS modifiers are different from the other nanofillers in a number of respects.[20] Structurally POSS units are precisely defined by their molecule architecture, unlike other nanofillers which can be relatively imprecisely defined structural units with distribution in both size and shape. A typical POSS molecule possesses the structure of cube-octameric frameworks represented by the formula ($R_8Si_8O_{12}$) with an inorganic silica-like core (Si_8O_{12}) surrounded by eight organic corner groups such as alkyl, aryl, or any of their derivatives[21,22] one or more of which is reactive or polymerizable.[23] Changing the nature and/or the size of the functional unit allows the generation of enormous number of POSS-based molecules with outer units of different character. Scheme 1 shows a representation of a POSS molecule with R attachments at all eight corners (R = cyclopentyl, cyclohexyl, etc.).[7] Generally, POSS cages can be incorporated into polymers via copolymerization and physical blending.[17−19]

*Corresponding author: Tel +86-21-54743268; Fax +86-21-54747445; e-mail zxshi@sjtu.edu.cn.

Scheme 1. POSS Macromonomer Structure

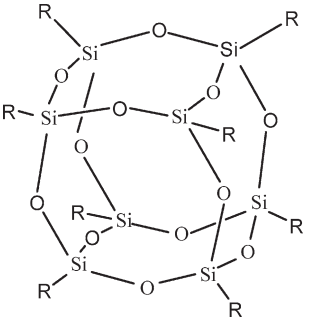

Copolymerization is an efficient approach to POSS-containing nanocomposites due to the formation of chemical bonds between POSS cages and polymer matrix. POSS unit can be covalently incorporated into large molecules by incorporating one (or more) chemically reactive group to specific corners of the cage to provide sites for further chemical reaction. During the past years, the ample literatures on the POSS containing copolymers[8] including polyethylene,[9] polyurethane,[11,24] epoxy thermosets,[12,25−32] polyimide,[33−36] and polybutadiene[37,38] have appeared, which represent a new generation of polymeric materials lying at the interface of organic and inorganic materials. These copolymers have superior mechanical properties (modulus, strength, etc.), higher glass transition temperatures, and superior fire resistance than the corresponding homopolymers.[39−42]

Polybenzimidazole (PBI) is a kind of aromatic heterocyclic polymers containing benzimidazole units. It is resistant to strong acids, bases, and high temperatures (up to 500 °C).[43] Because of

Published on Web 07/20/2010

these unique properties, PBI has been used to form membranes,[44] electrically conductive materials,[45] fire-resistance materials,[46] ultrafilters,[47] and other types of separatory media. In order to improve the mechanical properties of PBI, several kinds of inorganic fillers such as montmorillonite, etc., have been incorporated into the PBI matrix, but the reinforcement effect is not satisfactory.[48] Considering of the chemically reactive group of the POSS, we wonder whether the POSS with proper R group can be incorporated into PBI to prepare POSS reinforced PBI. Inspired by the method for the modification of carbon nanotubes based on the Friedel−Crafts (F−C) reaction using poly(phosphoric acid) (PPA/P_2O_5) as solvents proposed by the Tan research group,[49] we selected the octaphenyl-POSS, which could provide reactive sites for F−C reaction between phenyl group of the POSS and carboxylic acid monomer. By this way, POSS molecules could be successfully tethered to the PBI chain during the process of polymerization.

Recently, our research group has successfully prepared the soluble poly[2,2′-(*p*-oxidiphenylene)-5,5′-bibenzimidazole] (OPBI) in PPA/P_2O_5 (a kind of mild protonated acid).[50] Good solubility of

Scheme 2. Structure of Octaphenyl-POSS

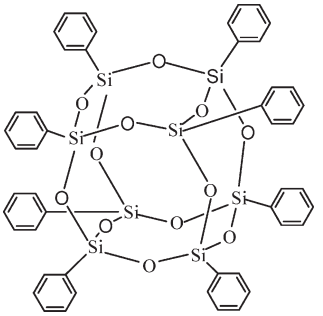

Scheme 3. Preparation of the Nanocomposites Containing Octaphenyl-POSS

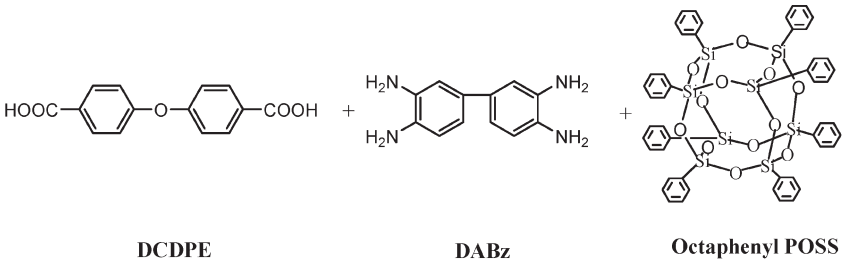

such polymers in high polar solvent makes it a potential candidate suitable for the preparation of POSS/OPBI polymers in one-pot synthesis, where F−C reaction of OPBI and POSS and polymerization could be combined together to be carried out simultaneously in one pot. In fact, it is found that the covalent linkage between POSS and polymer can be actually formed based on F−C reaction between phenyl groups from POSS and carboxylic acid from the monomer in PPA as medium. To the best of our knowledge, there has been no precedent report on OPBI/POSS nanocomposites based on this novel method. In the present work, we reported the preparation of OPBI/POSS nanocomposites, where octaphenyl-POSS was incorporated into polymer via the formation of covalent bonds using the PPA/P_2O_5 as medium. For comparison, the OPBI/POSS hybrids via physical blending were also obtained. The morphology and thermomechanical properties of two types of organic−inorganic hybrid composites are comparatively investigated on the basis of nuclear magnetic resonance (NMR), tensile test, scanning electronic microscopy (SEM), X-ray diffraction, dynamic mechanical analysis (DMA), and the thermogravimetric analysis (TGA).

2. Experimental Section

Materials. Octaphenyl polyhedral oligomeric silsesquioxane (octaphenyl-POSS) was purchased from Sigma-Aldrich. 3,3′-Diaminobenzidine (DABz) was purchased from J&K Chemical in Shanghai and used without further purification. 4,4′-Dicarboxydiphenyl ether (DCDPE) was kindly supplied by Peakchem (Shanghai) and vacuum-dried at 80 °C prior to use. Phosphorus pentoxide, poly(phosphoric acid) (PPA), and dimethyl sulfoxide (DMSO) were purchased from Sinopharm Chemical Reagent Co., Ltd. (SCRC). DMSO was distilled under reduced pressure and dried over 4A molecular sieves before use. Other materials were used as received.

Measurements. ^{1}H NMR spectra were recorded on a Varian Mercury Plus 400 MHz instrument. SEM was used to observe the phase structure of POSS-containing OPBI hybrids; all specimens were examined with a Hitachi S210 scanning electron microscope (SEM) at an activation voltage of 25 kV. The morphology of the cryo-fractured surface of composite was obtained using FE-SEM (JSM-7401 F, JEOL Ltd., Japan). X-ray powder diffraction (XRD) spectra were acquired by D/max-2200/PC (Japan Rigaku Corp.) using Cu Kα radiation. X-ray photoelectron (XPS) spectra were recorded on an ESCALAB 250 spectrometer (VG Scientific) with Al Kα radiation (1486.6 eV). The dynamic mechanical tests were carried out on a dynamic mechanical thermal analyzer (DMTA) (MKIII, Reometric Scientific, Ltd. Co., UK) with the temperature range from 100 to 400 °C. The frequency used is 1.0 Hz and heating rate 10 °C/min. Thermogravimetric analysis (TGA) was performed in nitrogen with a Perkin-Elmer TGA 2050 instrument at a hearting rate of 20 °C/min. For each measurement the sample cell was maintained at 100 °C for 30 min to evaporate the absorbed water in the sample before test. Tensile measurements were performed with an Instron 4465 instrument in ambient atmosphere at a crosshead speed of 5 mm/min.

Polymerization of POSS-*g*-OPBI/OPBI Nanocomposties. To a 100 mL dry three-neck flask equipped with a mechanical stirring device were added 45 g of PPA and 4.5 g of phosphorus pentoxide under nitrogen flow. The mixture was heated and stirred until phosphorus pentoxide was completely dissolved. After cooling to room temperature, 1.0713 g (0.5 mmol) of DABz, 1.2912 g (0.5 mmol) of DCDPEDS, and different amounts of POSS (1, 2, and 5 wt %) were added to the reaction flask. The reaction mixture was stirred and heated at 150 °C for 4 h and 190 °C for 20 h, respectively. Upon cooling, the gel-like mixture was transferred to ice water with stirring, and the precipitate was filtered off. The solid was soaked in 5% sodium bicarbonate solution for 2 days, then filtered, thoroughly washed with deionized water, and dried in vacuum at 120 °C for 10 h.

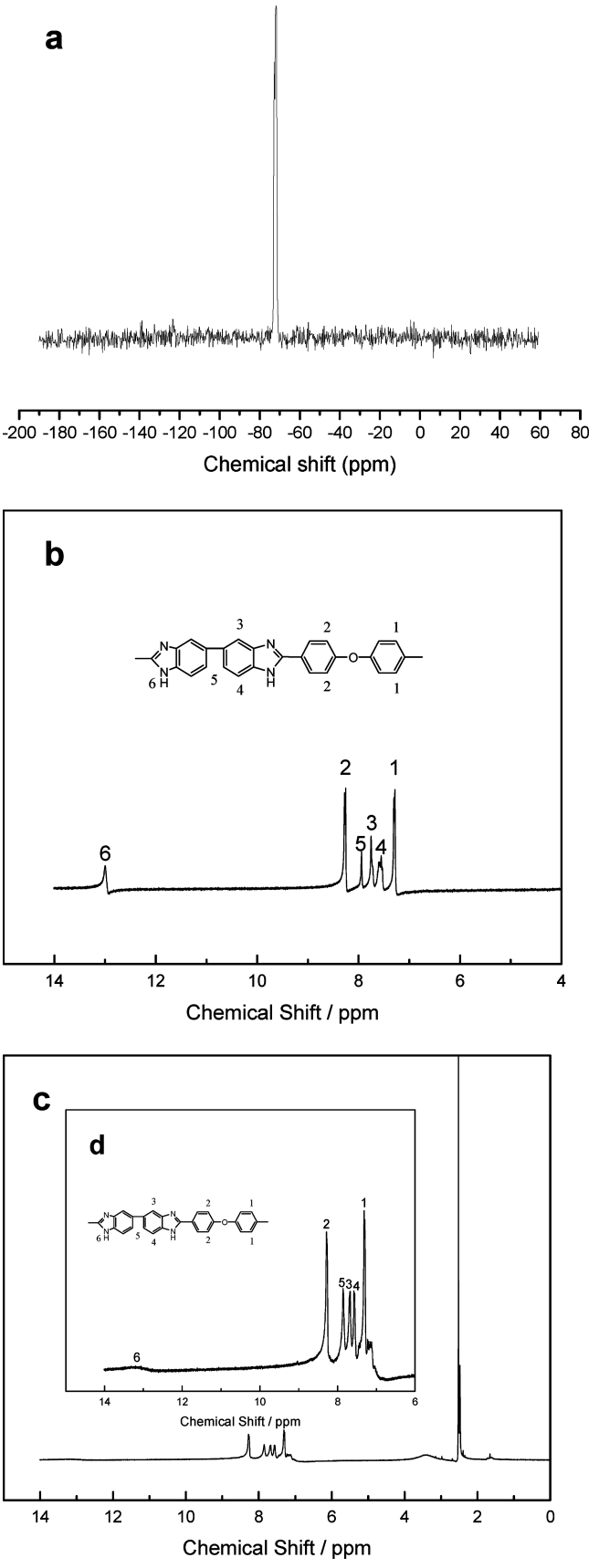

Figure 1. (a) Solid ^{29}Si CP/MAS NMR spectra of POSS-*g*-OPBI. ^{1}H NMR spectra of (b) OPBI, (c) POSS-*g*-OPBI, and (d) magnification of part of (c).

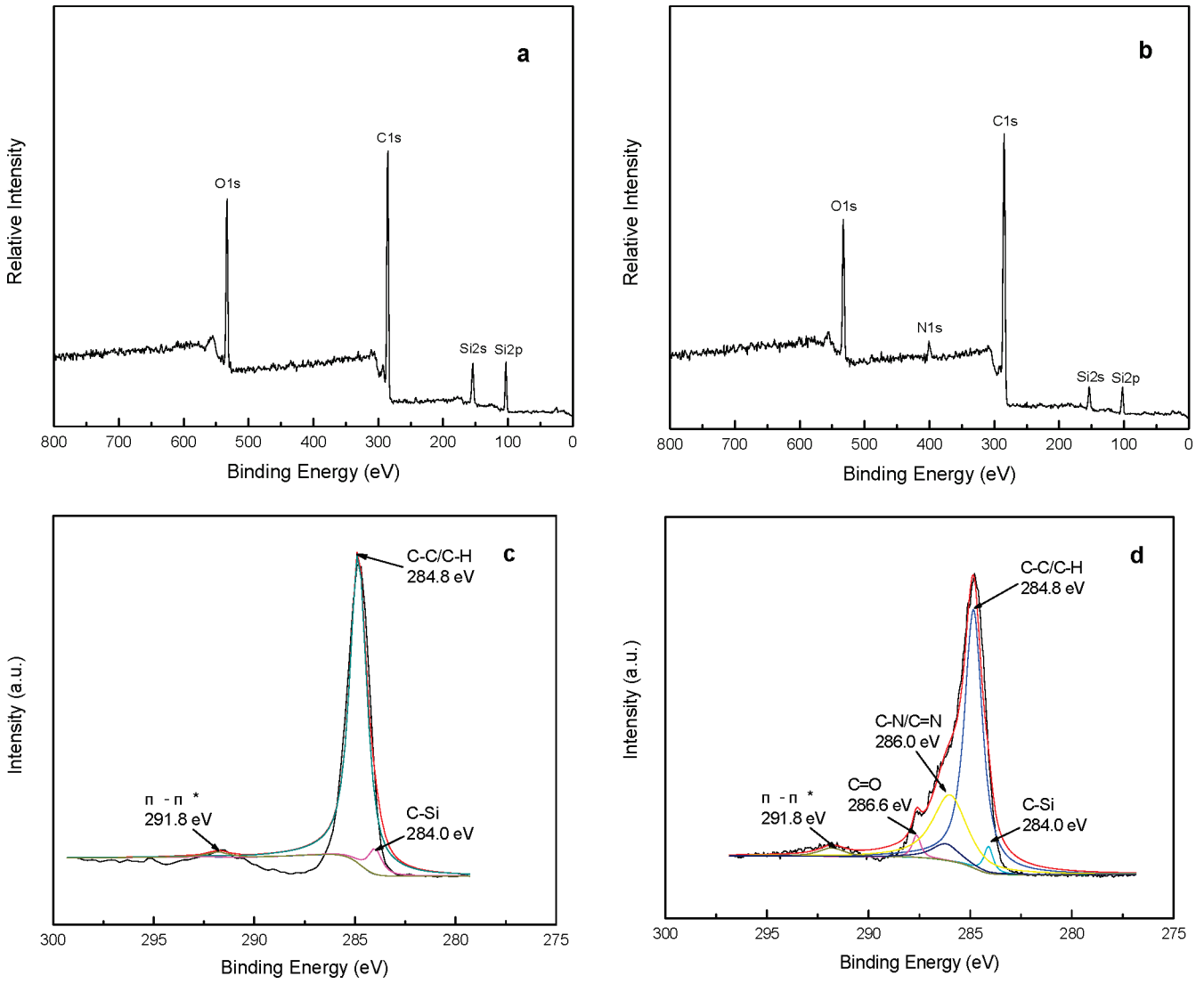

Figure 2. XPS spectra: (a) wide scan spectrum and (c) C 1s narrow scan spectrum of octaphenyl-POSS; (b) wide scan spectrum and (d) C 1s narrow scan spectrum of POSS-*g*-OPBI.

For comparison, OPBI was prepared without adding POSS in the same procedure as above. The silk-like product was brown, and the yield was about 96% (2.268 g).

Preparation of POSS Blending OPBI Hybrids. To a 50 mL dry two-neck flask was added 10 mL of DMSO and different amounts of POSS (1, 2, and 5 wt %). The mixture was magnetically stirred under nitrogen flow in an ultrasonic bath for 1 h, and then OPBI was added into the flask. The mixture was magnetically stirred at 80 °C for 12 h until the OPBI was completely dissolved in the DMSO. Upon cooling, the mixture was transferred to ice water with stirring and the precipitate was filtered off. The solid was thoroughly washed with deionized water and dried in vacuum at 120 °C for 10 h.

Membrane Formation. Polymer solution of 5−10 wt % in DMSO was sonicated for 15 min and then casted onto glass plates and dried in an air oven 80 °C for 5 h. The films were peeled off from glass plate and dried in vacuum at 120 °C for 10 h, followed by washing in water at 60 °C for 12 h to remove the residue solvent.

3. Results and Discussion

Reaction between OPBI and POSS. At the beginning, POSS-grafted-OPBI, which was obtained from the nanocomposites by removing the ungrafted OPBI, was subjected to ^{29}Si NMR measurement (Figure 1a) in order to investigate the stability of POSS in such acidic reaction media. It is found that only one peak at −71.8 ppm, which is characteristic resonance for POSS, was observed. Such results indicated that POSS were stable in PPA solvent without degradation. Thus, on the basis of the analysis of ^{29}Si NMR, it is concluded that its cage structure for POSS did not undergo any noticeable rearrangement in our selected reaction environment.

The chemical structure of POSS-*g*-OPBI was further confirmed by ^{1}H NMR. The ^{1}H NMR spectra of POSS-*g*-OPBI in deuterated DMSO are shown in Figure 1c. POSS-*g*-OPBI shows a good solubility in DMSO to form the homogeneous solutions, which is an important factor for successful NMR measurements. Resonances observed at 7.31, 7.56, 7.75, 7.94, 8.26, and 13.01 for the POSS-*g*-OPBI are readily assigned to the corresponding resonances of the neat OPBI. Compared of these spectra of pure OPBI and POSS-*g*-OPBI, we can also find that proton signals corresponding to the POSS-*g*-OPBI are broader and lower intensities, which is similar to the results reported in the NMR characterization of solubilized OPBI-grafted MWNTs.[51,52] Such comparison indicated the OPBI chains have been successfully attached to the POSS via the F−C reaction between phenyl groups of the POSS and carboxylic acid groups in OPBI.

XPS was then employed to elucidate the compositions of nanocomposites POSS and POSS-*g*-OPBI, as shown in Figure 2.

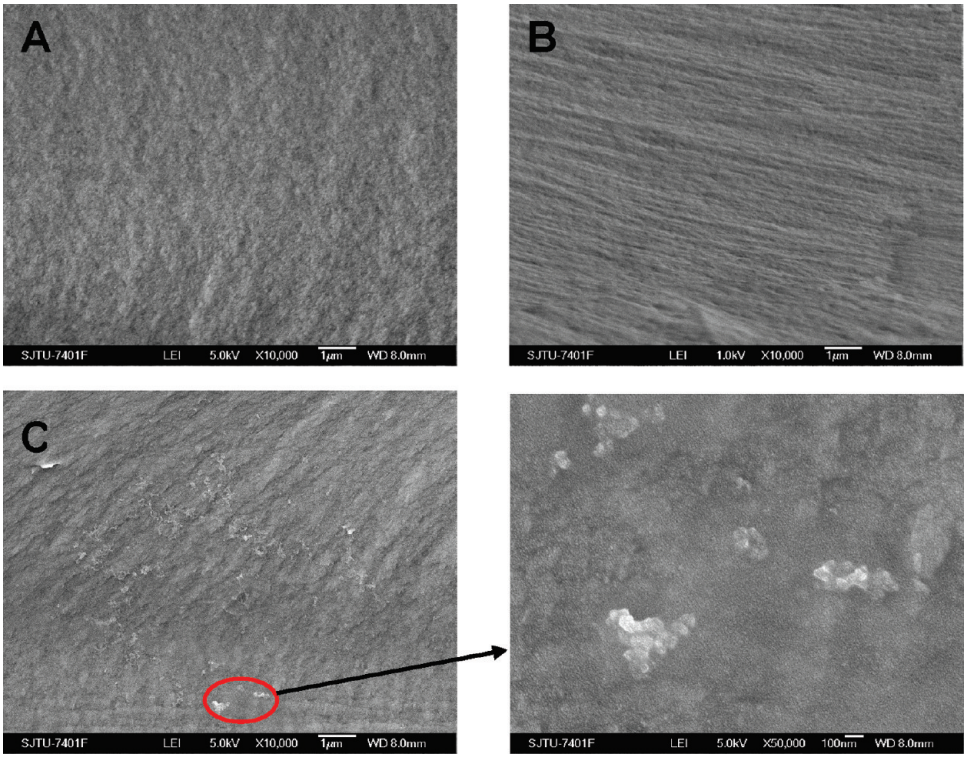

Figure 3. SEM images: (A) OPBI; (B) 5% POSS-*g*-OPBI; (C) 5% POSS blending.

The characteristic peaks for the POSS (a) are 285 eV for C 1s, 533 eV for O 1s, and two small peaks at 102 and 154 eV which are the characteristic peaks of Si 2p and Si 2s. The spectrum for POSS-*g*-OPBI (b) exhibited an additional new peak at 401 eV for N 1s as compared to POSS. The N 1s peak came from the imidazole group of the OPBI,[53] revealing the successful grafting of OPBI chains to POSS.

The peak components for C 1s peaks in the XPS spectra were further analyzed and the core level spectra are showed in (c) and (d). Both (c) and (d) display peak intensity at 284.1, 284.8, and 291.8 eV, corresponding to C−Si, C−C/C−H, and $\pi-\pi^*$ satellite species, respectively.[54] For the POSS-*g*-OPBI (d), the new peaks occurred at 287.6 eV (assigned to C═O) and 286 eV (assigned to C═N and C−N), indicating that OPBI chain has been successfully grafted to POSS. Detailed analysis of the XPS spectra provides clear evidence for the grafting of OPBI to POSS has been successfully achieved morphology of nanocomposites.

SEM was applied to characterize the fracture surface of POSS/OPBI nanocomposites to evaluate the dispersion of POSS in OPBI matrix. Figure 3 shows the fracture surface (broken under liquid nitrogen) of OPBI/POSS hybrids and physical blending with 5 wt % POSS loading (as a typically representive sample). It is found that the fracture surface of the 5% POSS-*g*-OPBI composite (Figure 3B) exhibited homogeneous dispersion without any discernible phase separation, and it is difficult to detect POSS in the fracture surface since POSS is totally embedded in the OPBI matrix. However, for the physical blending, POSS did not disperse well in OPBI matrix and was aggregated to form grains with sizes of ~100 nm. Such poor dispersion is related with the incompatibility between OPBI and POSS. Therefore, by comparison of fracture surfaces from OPBI/POSS hybrids and physical blending, a big difference in dispersion of POSS was obtained by two different methods, and the reaction between POSS and OPBI played a vital role in prevent the formation of POSS aggregates, leading to good dispersion of

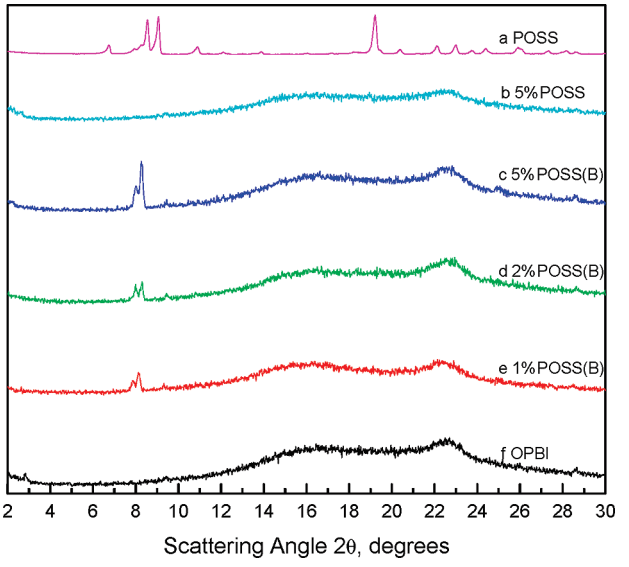

Figure 4. Diffractograms of POSS monomers, POSS/OPBI nanocomposites, and OPBI.

POSS in OPBI matrix. Such good dispersion would account for different mechanical and thermal properties for these two samples as will be discussed later.[34,35]

XRD. The wide-angle X-ray diffraction (WAXRD) measurements between 2° and 30° were applied to examine the crystalline structure of nanocomposites. The diffraction patterns of POSS-*g*-OPBI/OPBI are shown in Figure 4. For comparison, the XRD curve of POSS blending OPBI was also incorporated in this figure, which was measured under the identical condition.

The diffractogram of the pure POSS (a) showed very intense, characteristic POSS crystalline peaks at 8.56° (equivalent to an interplanar spacing of 10.3 Å), 9.06° (9.8 Å), and 19.22° (4.6 Å),

indicating that POSS is highly crystalline.[20,55] For the pure OPBI, the XRD pattern usually showed broad peaks from 10 to 26 Å, a characteristic amorphous structure. In addition to the amorphous broad peaks, two small diffraction maximum around $2\theta = 8.02$ and $2\theta = 8.26$ were observed for all the POSS blending OPBI polymers (c−f). The intensity of these peaks increased with increasing POSS loading. It was reported that such two diffraction peaks are due to the aggregation of POSS blocks in the polymer matrix.[56] By contrast, these intense reflections could not be observed in POSS-*g*-OPBI/OPBI nanocomposites containing 5 wt % POSS-*g*-OPBI (b), which showed that POSS were dispersed in the OPBI chains at nanometer scale without aggregation, consistent with the results obtained from SEM image analysis.

Mechanical Properties of the Nanocomposites. It was reported that the introduction of POSS modifiers into the other polymer matrix could improve its mechanical properties obviously, if POSS is dispersed well in a matrix.[8−12] The stress−strain curves of POSS reinforced OPBI composite prepared via F−C reaction are shown in Figure 5a. The Young's modulus, tensile strength, toughness, and ultimate strain of the composites are given in Table 1. Composites of OPBI−POSS via physical blending were also studied for comparison, and their stress−strain curves and mechanical properties are shown in Figure 5b and Table 2. The addition of as-received POSS improved the Young's modulus and yield stress. However, the degree of enhancement is not as good as that brought via F−C reaction. In the meantime, the addition of as received POSS into OPBI reduces the tensile strength, ultimate strain, and toughness. On the other hand, composites, prepared by F−C reaction, showed much better reinforcing effect with the incorporation of POSS. As the POSS content is increased to 2 wt %, the tensile strength is increased from 147.2 to 259.6 MPa, almost 76% increase, and the yield strength also improved from 91.2 to 125.0 MPa, almost 31% improvement. More importantly, the elongation of break is also simultaneously increased from 55.8% to 74.9%, almost 34% improvement, which indicates that the ductility of OPBI is not compromised but improved by the addition of POSS, which is quite different from the traditional composites, where the ductility and toughness of polymer are usually reduced substantially upon the incorporation of inorganic reinforced agent.[57,58] Retention or even improvement in ductility and toughness can be achieved by the use of polymer-grafted inorganic agents. In the present study, POSS were tightly embedded in OPBI matrix by the covalent linkage to the OPBI via F−C reaction, and OPBI can act as an effective cross-linking sites for linking the OPBI chains. As a result, the mechanical properties of OPBI were improved substantially due to a more efficient stress transfer from the matrix to POSS. Further increase in POSS content does not produce further improvement in the mechanical performance. Nevertheless, an effective POSS content of 2 wt % is sufficient to enhance the mechanical performance of OPBI.

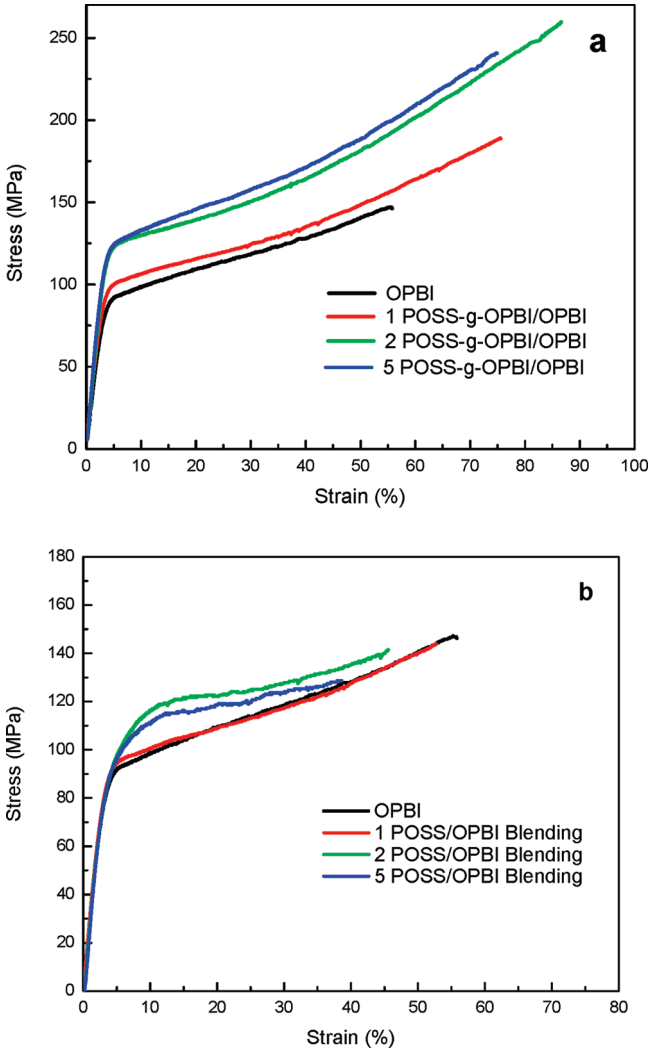

Figure 5. Selected representative stress−strain curves: (a) POSS-*g*-OPBI/OPBI nanocomposites; (b) POSS/OPBI blending hybrids.

Thermomechanical Properties. Shown in Figure 6 are the dynamic mechanical spectra for the control OPBI and its OPBI nanocomposites containing 1, 2, and 5 wt % POSS. In the plots of tan δ as functions of temperature, OPBI exhibits a well-defined relaxation peak centered at ca. 321.66 °C, which is assigned to the glass−rubber transition of the OPBI.

Table 2. Thermal Stability of OPBI Hybrid Composites Containing POSS

	T_d (°C)[a]	
POSS (wt %)	POSS-*g*-OPBI/OPBI (°C)	POSS (blending) (°C)
0	584.9	
1	594.1	
2	593.2	
5	597.8	557.1
100	437.3	

[a] Temperature at mass loss of 5 wt % under a N_2 atmosphere.

Table 1. Mechanical Properties of the Nanocomposites

samples	Young's modulus (GPa)	tensile strength (MPa)	elongition at break (%)	toughness (MPa)
OPBI	2.95 ± 0.08	147.2 ± 10.5	55.8 ± 9.0	63.6 ± 13.6
1% POSS-*g*-OPBI/OPBI	3.28 ± 0.11	189.0 ± 9.3	75.6 ± 2.9	75.5 ± 5.59
2% POSS-*g*-OPBI/OPBI	3.51 ± 0.14	259.6 ± 20.0	86.6 ± 5.4	151.5 ± 14.4
5% POSS-*g*-OPBI/OPBI	3.70 ± 0.06	240.7 ± 14.8	74.9 ± 6.1	127.3 ± 15.1
1% POSS/OPBI blend	3.35 ± 0.09	144.0 ± 11.6	52.7 ± 8.5	59.2 ± 12.6
2% POSS/OPBI blend	3.33 ± 0.08	141.3 ± 10.2	45.6 ± 3.2	53.8 ± 4.6
5%POSS/OPBI blend	3.29 ± 0.12	128.5 ± 12.9	38.6 ± 4.3	42.7 ± 5.7

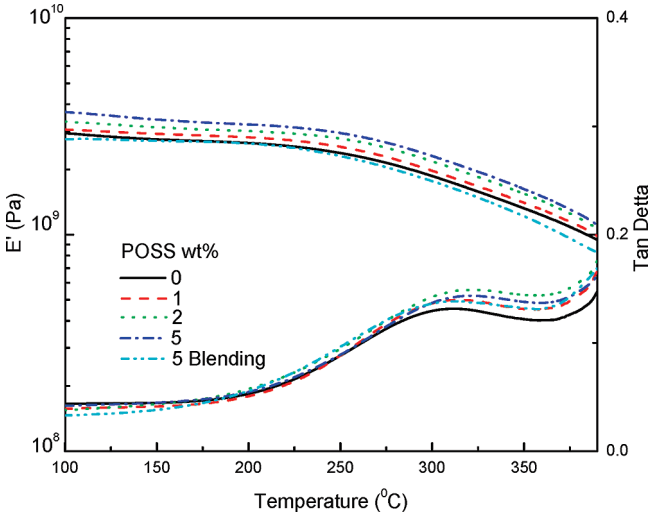

Figure 6. DMA mechanical spectra for OPBI nanocomposites containing POSS.

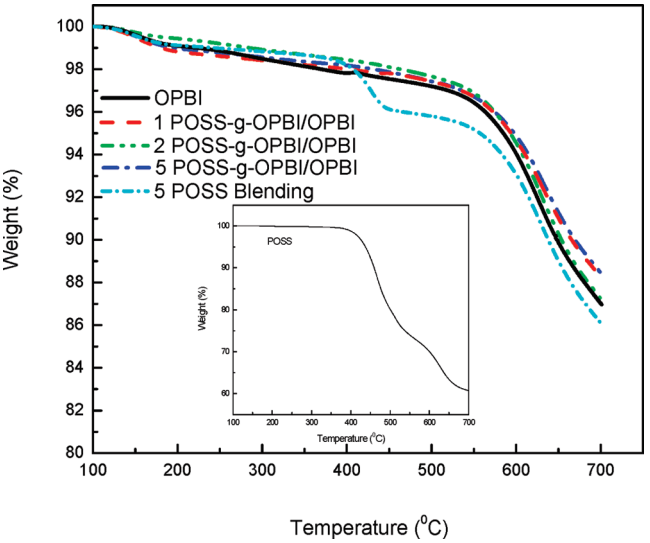

Figure 7. TGA curves of the OPBI and nanocomposites: (a) OPBI; (b) 1% POSS-*g*-OPBI/OPBI; (c) 2% POSS-*g*-OPBI/OPBI; (d) 5% POSS-*g*-OPBI.

The dynamic mechanical spectra of the nanocomposites containing 1, 2, and 5 wt % octaphenyl-POSS also display the single α transitions at ca. 321.7, 321.0, and 317.1 °C on the internal friction (tan δ) versus temperature curves, which could be related to the glass−rubber transition of the OPBI phase. It is found that T_g's for all the hybrid composites are lower than that of the OPBI. This observation implies that the inclusion of POSS gives rise to the increase of free volume of systems, which facilitates the motion of the OPBI chains.

Plots of storage modulus as functions of temperature for the OPBI and the OPBI nanocomposites containing 1, 2, and 5 wt % octaphenyl-POSS are also shown in Figure 6. It is interesting to note that the dynamic storage moduli of all POSS-containing nanocomposites were significantly higher than that of the OPBI, which is attributed to the nanoreinforcement provided by POSS due to its good dispersion in OPBI matrix via the covalent bonding between POSS and OPBI. The modulus increased with increasing the concentration of octaphenyl-POSS, consistent with the trends obtained by means of film stretching test. However, the physical blending sample with 5 wt % octaphenyl-POSS possessed the lower storage moduli of glassy and rubbery states than the control OPBI, which is in marked contrast to the sample prepared via F−C reaction. Such difference may be related with the poor dispersion of POSS in the physical blending, where the aggregation of POSS (as shown in Figure 3) deteriorated the mechanical properties of OPBI. By the chemical covalent linkage chemistry approach, POSS blocks were homogeneously dispersed in OPBI matrix at the nanoscale. Therefore, the incorporation of the nanometer-sized POSS blocks in the OPBI matrix brings about the significantly reinforcement of local chain.[59]

Therefore, different dispersion states will lead to different mechanical behaviors. For the nanocomposites prepared via F−C reaction, POSS was covalently linked to the OPBI chain and embedded tightly into in the OPBI matrix. Such strong interface interaction and good dispersion will lead to the obvious improvement in the mechanical properties for OPBI, especially, increase in tensile strength accompanied by the improvement of ductility. Such a phenomenon is not observed in the conventional organic−inorganic reinforced composites.

Thermal Stability. TGA was applied to evaluate the thermal stability of the POSS-grafted OPBI composites. Show in Figure 7 are the TGA curves of OPBI, POSS, and their composites recorded in N_2 atmosphere at 20 °C/min. For the neat POSS, the initial decomposition temperature that was defined as 5% mass loss temperature is 437.4 °C (in the rectangle circle of Figure 7). For the OPBI, the initial decomposition occurred at 584.9 °C. Thus, the thermal stability of POSS is lower than OPBI. As expected, the physical blending shows the lower thermal stability than the pure OPBI with the incorporation of the POSS. However, the 5% mass loss temperature for POSS-grafted hybrids is recorded at 594.1, 593.2, and 597.8 °C for 1, 2, and 5 wt % POSS-*g*-OPBI, respectively, almost 10 °C increasement. Such results imply that the thermal stability of the composites was improved by the presence of POSS, which is closely related with the dispersion of POSS in the OPBI matrix and their interaction. Since OPBI was covalently linked with POSS via F−C reaction, POSS was heavily coated with OPBI chains which protect the POSS from thermal degradation. In the meantime, POSS can also act as a cross-linking sites for OPBI chain. Both of these two factors may explain the improvement in the thermal stability for OPBI with the presence of the POSS.

4. Conclusion

A facile method to prepare the POSS-reinforced OPBI nanocompostites is established by initiating the polymerization of DCDPE and DABz in the presence of octaphenyl-POSS. POSS units were incorporated in the OPBI matrix via F−C reaction. NMR, XPS, and XRD measurements show that the covalent bonding between POSS and OPBI was successfully formed, which resulted in the good dispersion of POSS in OPBI matrix as evidenced by SEM. In the meantime, POSS can display a highly effective reinforcement toward to the OPBI matrix. Upon the addition of only 2 wt % POSS, the Young's modulus, tensile strength, and toughness are all improved by 31, 76, and 138.2%, respectively. More importantly, the ductility for the composites is not reduced but improved, which overcomes the brittleness brought by the addition of inorganic reinforced agent, a traditional shortcoming. Also, the thermal stability for OPBI is improved with the presence of POSS.

Acknowledgment. The authors thank the National Nature Science Foundation of China (No. 50973062) for the support. Additionally, the authors also acknowledge the staff of Instrumental

Analysis Center of Shanghai Jiao Tong University for the measurements. The support from Instrument Analysis Center of SJTU is also acknowledged.

References and Notes

(1) Whitesides, G. M.; Mathias, T. P.; Seto, C. T. *Science* **1991**, *254*, 1312–1319.
(2) Lan, T.; Kaviratan, P. D.; Pinnavaia, T. J. *Chem. Mater.* **1995**, *7*, 2144–2150.
(3) Giannelis, E. P. *JOM. F.* **1992**, *44*, 28–30.
(4) Theng, B. K. G. *Formation and Properties of Clay-Polymer Complexes*; Elsevier: Amsterdam, 1979.
(5) Mantz, R. A.; Jones, P. F.; Chaffee, K. P.; Lichtenhan, J. D.; Gilman, J. W.; Ismail, I. M. K.; Burmeister, M. J. *Chem. Mater.* **1996**, *8*, 1250–1259.
(6) Schwab, J. J.; Lichtenhan, J. D. *Appl. Organomet. Chem.* **1998**, *12*, 707–713.
(7) Feher, F. J.; Wyndham, K. D.; Baldwin, R. K.; Soulivong, D.; Lichtenhan, J. D.; Ziller, J. W. *Chem. Commun.* **1999**, *14*, 1289–1290.
(8) Li, G.; Wang, L.; Ni, H.; Pittman, C. U. *J. Inorg. Organomet. Polym.* **2001**, *11*, 123–154.
(9) Zheng, L.; Farris, R. J.; Coughlin, E. B. *Macromolecules* **2001**, *34*, 8034–8039.
(10) Xu, H.; Kuo, S. W.; Lee, J. S.; Chang, F. C. *Macromolecules* **2002**, *35*, 8788–8793.
(11) Fu, B. X.; Zhang, W. H.; Hsiao, B. S.; Rafailovich, M.; Sokolov, J.; Johansson, G.; Sauer, B. B.; Phillips, S.; Balnski, R. *High Perform. Polym.* **2000**, *12*, 565–571.
(12) Choi, J.; Harcup, J.; Yee, A. F.; Zhu, Q.; Laine, R. M. *J. Am. Chem. Soc.* **2001**, *123*, 11420–11430.
(13) Alan. J., Waddon.; Zheng, L.; Bryan Coughlin., E. *Nano Lett.* **2002**, *2*, 1149–1155.
(14) Zhang, C.; Babonneau, F.; Bonhomme, C.; Laine, R. M.; Soles, C. L.; Hristov, H. A.; Yee, A. F. *J. Am. Chem. Soc.* **1998**, *120*, 8380–8391.
(15) Kim, S. G.; Choi, J.; Tamaki, R.; Laine, R. M. *Polymer* **2005**, *46*, 4514–4524.
(16) Nair, M. B.; Blum, F. D. *Am. Chem. Soc. Polym. Prepr.* **2005**, *46*, 367–368.
(17) Phillips, S. H.; Haddad, T. S.; Tomczak, S. J. *Curr. Opin. Solid State Mater. Sci.* **2004**, *8*, 21–29.
(18) Madbouly, S. A.; Otaigbe, J. U. *Prog. Polym. Sci.* **2009**, *34*, 1283–1332.
(19) Cordes, D. B.; Lickiss, P. D.; Rataboul, F. *Chem. Rev.* **2010**, *110*, 2081–2173.
(20) Waddon, A. J.; Coughlin, E. B. *Chem. Mater.* **2003**, *15*, 4555–4561.
(21) Harrison, P. G. *J. Organomet. Chem.* **1997**, *542*, 141–183.
(22) Baney, R. H.; Itoh, M.; Sakakibara, A.; Suzuki, T. *Chem. Rev.* **1995**, *95*, 1409–1430.
(23) Ni, Y.; Zheng, S. X. *Chem. Mater.* **2004**, *16*, 5141–5148.
(24) Fu, B. X.; Hsiao, B. S.; Pagola, S.; Stephens, P.; White, H.; Rafailovich, M.; Sokolov, J.; Mather, P. T.; Jeon, H. G.; Phillips, S.; Lichtenhan, J.; Schwab, J. *Polymer* **2001**, *42*, 599–611.
(25) Lee, A.; Lichtenhan, J. D. *Macromolecules* **1998**, *31*, 4970–4974.
(26) Matejka, L.; Strachota, A.; Plestil, J.; Whelan, P.; Steinhart, M.; Slouf, M. *Macromolecules* **2004**, *37*, 9449–9456.
(27) Strachota, A.; Kroutilova, I.; Kovarova, J.; Matejka, L. *Macromolecules* **2004**, *37*, 9457–9464.
(28) Choi, J.; Kim, S. G.; Laine, R. M. *Macromolecules* **2004**, *37*, 99–109.
(29) Laine, R, M.; Choi, J.; Lee, I. *Adv. Mater.* **2003**, *13*, 800–803.
(30) Choi, J.; Yee, A. F.; Laine, R. M. *Macromolecules* **2003**, *36*, 5666–5682.
(31) Choi, J.; Yee, A. F.; Laine, R. M. *Macromolecules* **2004**, *37*, 3267–3276.
(32) Abad, M. J.; Barral, L.; Fasce, D. P.; Williams, R. J. J. *Macromolecules* **2003**, *36*, 3128–3135.
(33) Wright, M. E.; Schorzman, D. A.; Feher, F. J.; Jin, R. Z. *Chem. Mater.* **2003**, *15*, 264–268.
(34) Choi, J.; Tamaki, R.; Kim, S. G.; Laine, R. M. *Chem. Mater.* **2003**, *15*, 3365–3375.
(35) Tamaki, R.; Choi, J.; Laine, R. M. *Chem. Mater.* **2003**, *15*, 793–797.
(36) Asuncion, M. Z.; Laine, R. M. *Macromolecules* **2007**, *40*, 552–562.
(37) Fu, B. X.; Lee, A.; Haddad, T. S. *Macromolecules* **2004**, *37*, 5211–5218.
(38) Zheng, L.; Hong, S.; Cardoen, G.; Burgaz, E.; Dido, S. P.; Coughlin, E. B. *Macromolecules* **2004**, *37*, 8606–8611.
(39) Ni, Y.; Zheng, S. X. *Chem. Mater.* **2004**, *16*, 5141–5148.
(40) Wu, S.; Hayakawa, T.; Kikuchi, R.; Grunzinger, S. J.; Kakimoto, M. *Macromolecules* **2007**, *40*, 5698–5705.
(41) Chou, C. H.; Hsu, S. L.; Yeh, S. W.; Wang, H. S.; Wei, K. H. *Macromolecules* **2005**, *38*, 9117–9123.
(42) Miyake, J.; Chujo, Y. *Macromol. Rapid Commun.* **2008**, *29*, 86–92.
(43) Vogel, H.; Marvel, C. S. *J. Polym. Sci.* **1961**, *50*, 511–518.
(44) Trouw, N. S. U.S. Patent 4,693,825, Sept 15, 1987.
(45) Akita, H.; Ichikawa, M.; Nosaki, K.; Oyanagi, H. U.S. Patent 6,124,060, Sept 26, 2000.
(46) Kasowski, R. V.; Lee, K.-S. U.S. Patent 5,389,326, Feb 14, 1995.
(47) Sansone, M. J. U.S. Patent 4,693,824, Sep 15, 1987.
(48) Choi, S. H.; Coronas, J.; Lai, Z. P.; Yust, D.; Onorato, F.; Tsapatsis, M. *J. Membr. Sci.* **2008**, *316*, 145–152.
(49) Baek, J. B.; Lyons, C. B.; Tan, L. S. *Macromolecules* **2004**, *37*, 8278–8285.
(50) Xu, H. J.; Chen, K. C.; Gao, X. X.; Fang, J. H.; Yin, J. *Polymer* **2007**, *48*, 5556–5564.
(51) Shao, H. Z.; Shi, Z. X.; Fang, J. H.; Yin, J. *Polymer* **2009**, *50*, 5987–5995.
(52) Zhao, B.; Hu, H.; Robert, C. H. *Adv. Funct. Mater.* **2004**, *14*, 71–76.
(53) Zeng, K.; Zheng, S. X. *J. Phys. Chem. B* **2007**, *111*, 13919–13928.
(54) Beamson, G.; Briggs, D. *High-Resolution XPS of Organic Polymers: The Scienta ESCA300 Database*; John Wiley: Chichester, UK, 1992.
(55) Brown, T. F., Jr.; Vogt, L. H., Jr.; Prescott, P. I. *J. Am. Chem. Soc.* **1964**, *86*, 1120.
(56) Ni, Y.; Zheng, S. X. *Macromolecules.* **2007**, *40*, 7009–7018.
(57) Tseng, C. H.; Wang, C. C.; Chen, C. Y. *Chem. Mater.* **2007**, *19*, 308–315.
(58) Yang, B. X.; Pramoda, K. P.; Xu, G. Q.; Goh, S. H. *Adv. Funct. Mater.* **2007**, *17*, 2062–2069.
(59) Liu, H. Z.; Zheng, S. X.; Nie, K. Z. *Macromolecules* **2005**, *38*, 5088–5097.